



# Preparation, characterization and comparative ionizing electromagnetic radiation performances: part I—metal oxide reinforced polymeric composites

E. Eren Belgin<sup>1</sup> · G. A. Aycik<sup>1</sup>

Received: 20 March 2020 / Published online: 15 June 2020  
© Akadémiai Kiadó, Budapest, Hungary 2020

## Abstract

Isophthalic polyester resin was reinforced by using different metal oxides (lead(II)oxide, tungsten(VI)oxide and ferric oxide) and different reinforcement ratios (10–50%). Ionizing electromagnetic radiation shielding performance of the composites were determined by gamma spectrometric techniques for three different ionizing electromagnetic radiation (IEMR) energy regions (60–392, 662–898, 1173–1836 keV). Density evaluation, FTIR analysis, SEM studies were carried out. The IEMR attenuation performances of the composites were determined with gamma spectroscopy and found to be satisfying. These composites give better performance with respect to reference lead, especially in the case of the applications that weight of IEMR shield is important.

**Keywords** Electromagnetic radiation shielding · Gamma shielding · Composite gamma shielding · Polymeric gamma shielding

## Introduction

Massless and uncharged ionizing electromagnetic radiation (IEMR) has enough energy to ionize atoms of the interacting matter and it has harmful effects on human and environment. The ALARA (As Low As Reasonably Achievable) radiation safety principle is based on the minimization of radiation doses and limiting the release of radioactive materials into the environment by employing reasonable methods. IEMR must be shielded by using appropriate shielding materials according to ALARA principles. High density materials are used as IEMR shields to increase interaction between IEMR and matter for reducing its intensity and the exposure dose. At the present time, lead is the most used shielding material due to its low cost, high density and atomic number for wearable, mobile and stationary shielding applications. Some other shielding materials are tungsten, copper, bismuth and steel, which are still in use but limited in use. However, lead shields has significant disadvantages that canalize scientist

for developing novel IEMR shielding materials as heaviness, low mechanic and chemical stability and toxicity.

Nowadays, composite materials are mostly studied because of their ability of combining different properties of the individual materials used for production of composite material. Polymers are desired as matrix material for this manner because of their low weight, high mechanical/chemical stability, cheapness, easy production methods and process ability. Different polymers can be chosen due to the application area of the shield providing needed properties as flexibility, UV stability, transparency etc. One of the most important points to be considered in the selection of polymer matrix is that the polymer used should not undergo degradation on gamma radiation. IEMR shielding performance of the polymer based composite materials are mostly improved by using reinforcement materials with high density. Epoxy-limonite [1], polymer-bismuth [2], lead-natural rubber [3, 4], lead-unsaturated polyester [5], poly(hydroxyethyl metacrylate)-tungsten(VI) oxide [6], hafnium/tungsten trioxide-epoxy [7], poly(vinyl alcohol)-bismuth oxide [8], UHMWPE-nano Bi<sub>2</sub>O<sub>3</sub> [9], isophthalic polymer-bismuth [10], boron carbide reinforced polymers [11], epoxy based [12] composites are some of studied polymer based composites for radiation shielding.

✉ E. Eren Belgin  
ebelgin@mu.edu.tr

<sup>1</sup> Chemistry Department, Muğla Sıtkı Koçman University, Kotekli Campus, 48000 Muğla, Turkey

In the present study, isophthalic unsaturated polyester (PES) was reinforced with three different metal oxide (lead (II) oxide, tungsten (VI) oxide and ferric oxide) and five different reinforcement ratios between 10 and 50%. PES was chosen as composite matrix for providing load-stress transfer while decreasing composite weight and composite raw material and processing cost. Formation of secondary radiation was also set down to minimum due to the hydrogen content of PES by generating many interaction points in the polymer and due to the lack of heavier atoms than carbon in the PES in contrast with lead. The function of metal oxide reinforcements increased IEMR shielding performance of the composites due to higher densities and atomic numbers than PES.

IEMR shielding performances were determined by gamma spectrometric methods at three different IEMR energy regions. These energy intervals were selected by considering the predominant IEMR-matter interaction mechanisms differing mainly according to IEMR energies that affects shielding performance of the composites, Table 1.

Studying at different energy regions also permit suggesting different composites for different application areas that radiation sources with different energies are used. Obtained results were compared for different composites and different reinforcement loading ratios.

Several characterization studies were also carried out for prepared composites. After density evaluation was done FTIR analysis were held for understanding nature of interaction between reinforcements and matrix of the composite. SEM studies were also carried out for morphological examination of composites.

## Experimental

### Constituents of the composites

Composite matrix PES ( $1.15 \text{ g cm}^{-3}$ ) with low volumetric shrinkage is a thermoset resin in styrene monomer. Styrene

**Table 1** Predominant IEMR-matter interaction mechanisms at different IEMR energies

IEMR energy	Predominant interaction mechanism	Relationship with atomic number (Z) of absorber material
Low (especially for energies < 400 keV)	Photoelectric effect	$Z^5$
Intermediate	Compton scattering	Z
High (especially for energies > 1.02 MeV)	Pair production	$Z^2$

decreases viscosity of the resin and allows preparation of a homogeneous composite mixture including reinforcement materials, catalyst and initiator. The PES resin, the initiator (MEKP: methyl ethyl ketone peroxide) and the catalyst (Coct: cobalt octoate) used for composite production were procured commercially.

Three different reinforcement materials were used for composites. Their properties are given in Table 2.

### Preparation of the composites

Formation of crosslinks within PES resin was performed with free-radical polymerization process by using methyl ethyl ketone peroxide as the radical source and cobalt octoate (Coct) catalyst. Thus crosslinks that would led a rigid three dimensional lattice of the PES thermoset were formed. Resin mixtures were prepared by using five different filler loadings between 10 and 50%. Reinforcement materials were oven dried to the constant weight at  $110 \text{ }^\circ\text{C}$  temperature before weighing. Reinforcements and resin were weighed with a calibrated ( $10^{-3} \text{ g}$ ) electrical balance and reinforcement particles were mechanically dispersed (120 rpm) into the resin. Then 0.75% Coct and 1.25% MEKP were added to the resin and crosslinking process was started. In this step it was observed that if mixture is immediately poured into the mold the heavy reinforcement particles starts to precipitate at the bottom of the mold due to gravity. Thus mechanically mixing was continued until gelation point of the resin where viscosity of the mixture was increased due to crosslinking. Thus precipitation of the reinforcement particles was prevented. Then composite mixture was placed into a closed steel mold by overflowing. The composites were cured in the mold for 24 h at room temperature and eight hours at  $80 \text{ }^\circ\text{C}$  constant temperature for completion of the polymerization.

### Characterization of composites

#### Density evaluation and structural characterization of the composites

An Archimedes' density measurement equipment was used for evaluation of experimental densities of the composites. Theoretical values of the bulk densities of the composites were also calculated and compared with the experimental

**Table 2** Chemical properties of the used reinforcements

Reinforcement	Molecular weight	Density	Crystal structure
PbO (BDH)	$223.20 \text{ g mol}^{-1}$	$9.53 \text{ g cm}^{-3}$	Orthorhombic
WO <sub>3</sub> (Sigma Aldrich)	$231.84 \text{ g mol}^{-1}$	$7.16 \text{ g cm}^{-3}$	Monoclinic
Fe <sub>3</sub> O <sub>4</sub> (BDH)	$231.533 \text{ g mol}^{-1}$	$5 \text{ g cm}^{-3}$	Rhombohedral

values. Details of the experimental and theoretical density evaluation methods are previously described [13]. Nature of interaction between PES and reinforcements is examined by Fourier transform infrared spectrophotometer (FTIR-Thermo Scientific-Nicolet-1510) analysis. Morphological examination of composites was carried out by using scanning electron microscope (SEM-Jeol-JSM-7600F) for both fractured and polished surfaces of the composites. Dispersibility of reinforcement particles with PES, microstructure of the composites and binding behavior between reinforcement and matrix were examined by using SEM micrographs.

### IEMR attenuation performance measurements

IEMR attenuation performances of the composites were determined via gamma spectrometric measurements by using a 110 cm<sup>3</sup> well-type HPGe detector coupled with a 64 k channel analyzer. The system had a resolution of 3.78 keV at 1.33 MeV gamma-ray peak of Co-60. The detector was housed in a lead shielding 10 cm thick lined with 1.5 mm thick tin and 1.0 mm thick copper in order to reduce the X-ray interferences. Performance measurements were held for low (0–500 keV), intermediate (500–1100 keV) and high (> 1100 keV) IEMR energy regions for determination of usability of composites for shielding of different IEMR sources used in different application areas. A disc shaped standard mixed point gamma source (Eckert &

Ziegler-Mixed nuclide point source-QCRB1186) containing several radionuclides having photopeak energies between 60 and 1836 keV was used for measurements in this manner. Radionuclide content (that have clear photopeaks) of the source, photopeak energies and activities of the radionuclides are given in Table 3.

IEMR attenuation performance calculations were done relatively by comparing inlet and outlet radiation intensity of photopeaks to avoid any efficiency calibration errors. Inlet radiation intensity was measured by a blank measurement (measurement for only source without placing any other material between the source and detector) since knowing the gamma radiation intensity directly coming from the source would lead to calculate attenuation ratio of the materials. The geometrical arrangement of the measurement system is given in Fig. 1.

The data acquisitions were performed for a period of 1500 s that gives < 1% count error. The spectra were evaluated by using the Maestro-ORTEC software program. All the measurements were held three times and the mean values were used for the calculations.

After measurements were completed, percentage attenuation performances (F%), half value layers (HVL), linear ( $\mu_L$ ) and mass ( $\mu_M$ ) attenuation coefficients of the composites were calculated as it was given detailed in previous articles [13–15].

**Table 3** Mixed point source radionuclide content, their photopeak energies and activities considered in performance calculations

Radionuclide	Photopeak energy (keV)	Activity (kBq)	Overall uncertainty (%)
Am-241	60	3	3
Co-57	122	0.6	2.5
Ce-139	166	0.7	2.5
Hg-203	27	2.1	2.5
Sn-113	392	2.8	5
Cs-137	662	2.6	2.5
Y-88	898, 1836	5.9	4
Co-60	1173, 1332	3.0	1

## Results and discussion

### Density and microstructure of the composites

The composite designations, reinforcement loading percentages and densities of the prepared composites are summarized in Table 4.

Composite density was increased with increase reinforcement ratio for all reinforcement types. This is an expected result since density of the reinforcements (PbO: 9.53 g cm<sup>-3</sup>; WO<sub>3</sub>: 7.16 g cm<sup>-3</sup>; Fe<sub>3</sub>O<sub>4</sub>: 5.00 g cm<sup>-3</sup>) are higher than density of PES (1.15 g cm<sup>-3</sup>) (see Fig. 2).

The experimental and theoretical densities of the composites were compatible with each other. Maximum deviation

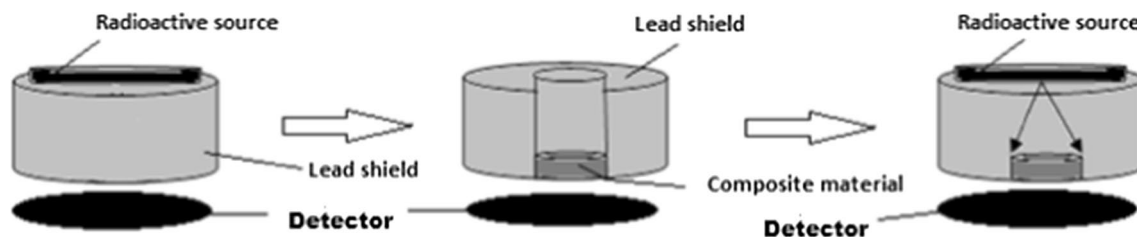


**Fig. 1** Geometric arrangement of IEMR attenuation measurement system

**Table 4** Sample designations, reinforcement loading percentages and experimental/theoretical densities of the prepared composites

Composite designation	Reinforcement	Reinforcement loading (%)	Experimental density (g cm <sup>-3</sup> )	Theoretical density (g cm <sup>-3</sup> )
1-PBO	PbO	10	1.30	1.26
2-PBO	PbO	20	1.45	1.40
3-PBO	PbO	30	1.59	1.56
4-PBO	PbO	40	1.87	1.77
5-PBO	PbO	50	2.12	2.05
1-WO	WO <sub>3</sub>	10	1.27	1.26
2-WO	WO <sub>3</sub>	20	1.33	1.38
3-WO	WO <sub>3</sub>	30	1.41	1.54
4-WO	WO <sub>3</sub>	40	1.74	1.73
5-WO	WO <sub>3</sub>	50	1.99	1.98
1-FEO	Fe <sub>3</sub> O <sub>4</sub>	10	1.31	1.25
2-FEO	Fe <sub>3</sub> O <sub>4</sub>	20	1.34	1.36
3-FEO	Fe <sub>3</sub> O <sub>4</sub>	30	1.54	1.50
4-FEO	Fe <sub>3</sub> O <sub>4</sub>	40	1.72	1.67
5-FEO	Fe <sub>3</sub> O <sub>4</sub>	50	1.85	1.88

was observed for 3-WO composite with approximately 8% difference between the values. These acceptable differences were thought to arise from weighing errors made during preparation of the composites and density evaluation experiments.

The maximum filler loading of 50% caused an increment in the density of the composite matrix (PES) approximately 84%, 73% and 61% for PbO, WO<sub>3</sub> and Fe<sub>3</sub>O<sub>4</sub> reinforcements, respectively. Increment in experimental densities was also showed that critical reinforcement loading is not exceed for composites. Because if critical loading value was exceeded, there couldn't be enough PES resin to surround surfaces of all reinforcement particles. This would cause formation of gaps in the structure that decreases density of the composites [5].

The micrographs determined by SEM studies for the polished and fractured surfaces of the 50% reinforced composites are shown in Fig. 3.

Reinforcement and PES were easily distinguished at the polished surfaces and phase separation at the reinforcement-PES interface was not observed. Homogeneous dispersion of reinforcement particles was one of the most important requirement for accurate results of the study. SEM micrographs showed a good dispersibility of the reinforcement within PES matrix.

The FTIR spectra of the 50% reinforced composites and composite matrix PES are given in Fig. 4.

Characteristic transmission bands (approximately 1720, 1240, 1015, 790 cm<sup>-1</sup>) of PES are seen in FTIR spectrum of PES in Fig. 4. The same positions of transmission band peaks were also represented by PES based composites are also seen at the FTIR spectra of all the composites. No significant difference in FTIR peak locations was found for

composites and pure PES. Percentage transmission value of these bands showed some differences due to possible bond density differences at the interested region of the analyzed sample. Thus FTIR studies indicated that there were no changes in chemical structure of polymer after addition of reinforcements.

## IEMR attenuation performances of the composites

### Effect of reinforcement loading ratio on IEMR attenuation performances

The determined F% values that represent percentage IEMR attenuation performances of the composites are given with respect to IEMR energy are given in Figs. 5, 6 and 7 for PbO, WO<sub>3</sub> and Fe<sub>3</sub>O<sub>4</sub> reinforced composites, respectively.

IEMR attenuation performances of all composites had an increasing tendency with increasing reinforcement loading ratio for all composites. The increment was due to increasing density of the composites. The sharpest increasing was observed between 0 and 500 keV IEMR energy that photoelectric effect is dominant interaction mechanism. Increasing behavior was continued as the IEMR energy increases but not as sharp as low energies. This was a compatible result because the predominant interaction mechanisms of photoelectric effect (0–500 keV), Compton scattering (500 keV–10 MeV) and pair production (> 1.022 MeV) are proportional with Z<sup>5</sup>, Z and Z<sup>2</sup>, respectively. Thus increasing density of the composites causes sharp increasing at low energies while increasing is smoother at higher energies.

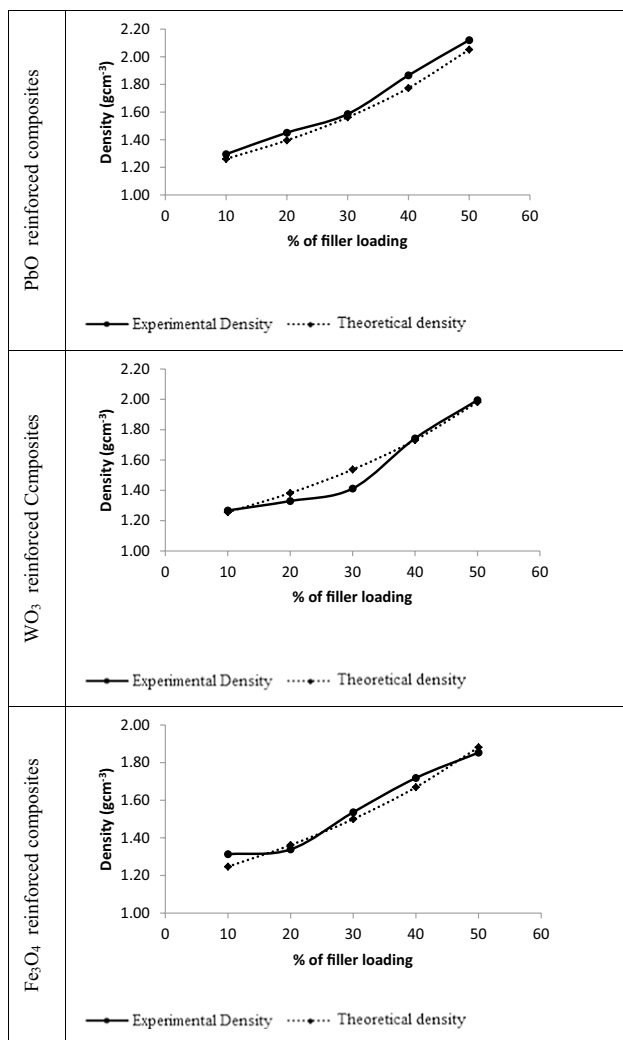


**Fig. 2** Variation of the theoretical and experimental values of densities with respect to filler loading

### Effect of the composite density on linear attenuation coefficients

The  $\mu_L$  values of the prepared composites showed a linear dependence on densities. This dependence is shown in Figs. 8, 9 and 10 for PbO, WO<sub>3</sub> and Fe<sub>3</sub>O<sub>4</sub> reinforced composites, respectively. Mean  $\mu_L$  values for low (mean of 60, 88, 122, 166, 392 keV results), intermediate (mean of 662, 898 keV results) and high (mean of 1173, 1332, 1836 keV results) energy regions are plotted in the figures for a more comprehensible comparison.

The interaction mechanisms of IEMR with matter differs due to energy of the IEMR as it was mentioned for F% values of the composites. The predominant interaction mechanisms differ due to IEMR energies and they are proportional with  $Z^5$  (low),  $Z$  (intermediate) and  $Z^2$  (high) at different IEMR energy regions [16]. Thus as the energy increases

dependence of attenuation on  $Z$  of interacting material decreases as it is seen Figs. 8, 9 and 10. In the study, the  $\mu_L$  values of the composites increased sharply with increasing density of the composites at low IEMR energy region, the density became ineffective on  $\mu_L$  values for intermediate energy region and a slightly insignificant increasing behavior observed for high energy region as it was expected.

### Effect of reinforcement type on linear attenuation coefficients

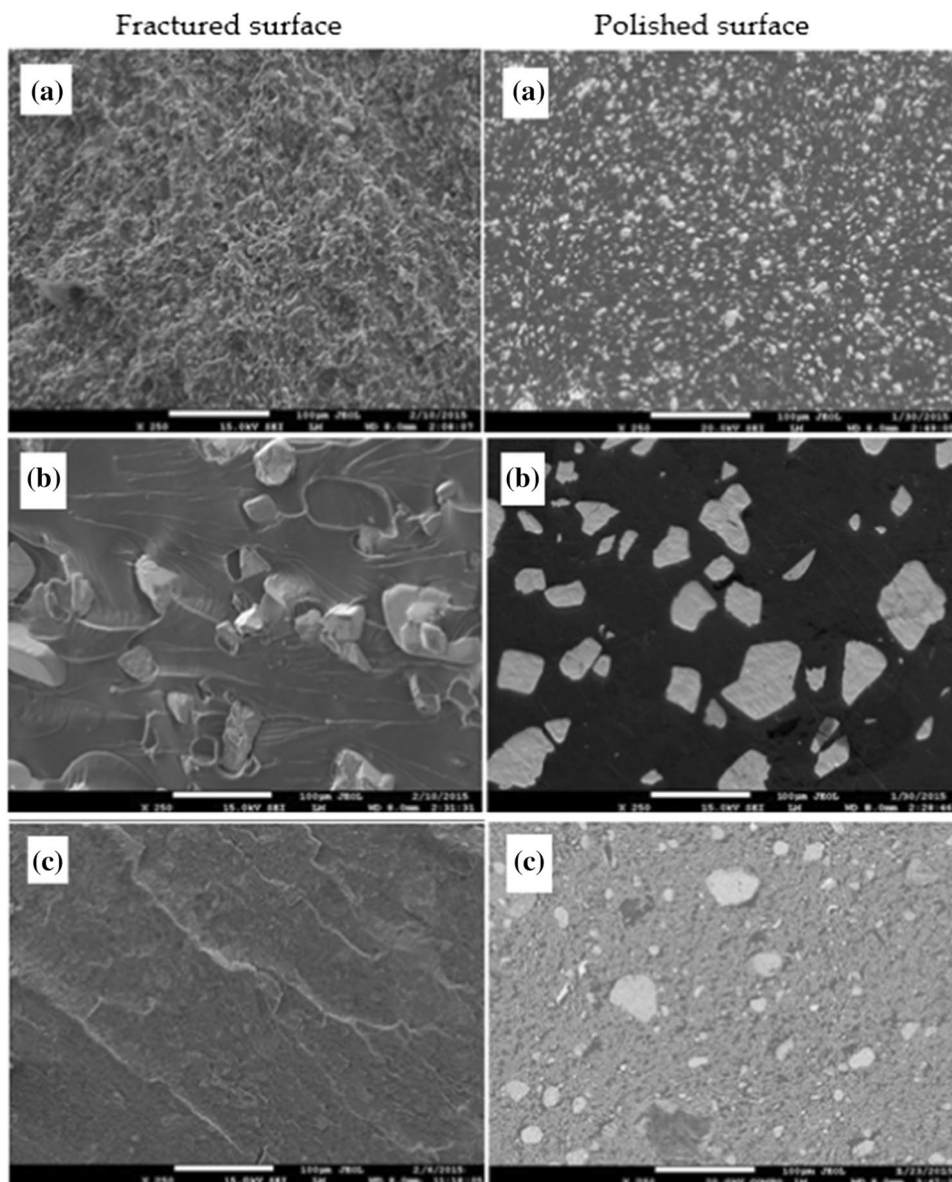
The absorber materials attenuate IEMR at different ratios according to their densities, molecular weights and crystal structures. The main factor for effective attenuation is that when IEMR passes through the material, it comes across the maximum number of atoms and atomic electrons. Thus, more energy is transferred to these atoms and IEMR exits from the material with low energy or attenuate totally. Thus as the reinforcement loading ratio increases (density increases) the probability of coming across of IEMR with an atom increases.

The crystal structure of the material is another property that effects this probability. If the crystal lattice structure of the material is close packed the IEMR attenuation probability increases. Crystal structures of all three reinforcements used in this study are the close packed lattice structures.

In Figs. 11, 12 and 13, the 50% reinforced composites' (showing the highest performances) and lead's  $\mu_L$  values are compared for low, intermediate and high energy regions, respectively.

Lead is an excellent IEMR shielding material due to its high density and closed packed crystal structure beside its important disadvantages as toxicity. Thus as it was expected, lead had higher  $\mu_L$  values, in other words higher attenuation performance for unit thickness, for all energy regions. On the other hand, 5-PBO composite reached approximately 76% performance of lead at low energy region and it was superior on lead with its approximately 5.5 times lower weight and non-toxic nature. The reinforcement PbO was still toxic but it was buried into PES thus composite was not toxic during utilization. If both of reinforcement and matrix is desired non-toxic, 5-WO could be proposed with its approximately 5.7 times lower weight and performance reaching approximately 35% performance of lead. The composite performances were not showed significant performance differences for intermediate and high energy regions as reason of it mentioned before. The composite with best performance was 5-FEO with its non-toxic nature and performance reaching approximately 21% and approximately 26% of lead performance, respectively at these regions. 5-FEO was also approximately 6 times lighter than lead and non-toxic that makes it advantageous.

**Fig. 3** SEM micrographs ( $\times 250$ ) of composite polished surfaces and fractured surfaces (a 5-PBO, b 5-WO, c 5-FEO)



### Effect of reinforcement type on mass attenuation coefficients

$\mu_M$  value that represent attenuation per gram of a shielding material is another important parameter especially when weight of the shield is important. In case of using shielding materials with high  $\mu_M$  values, higher performances can be achieved with a lighter shield. The determined  $\mu_M$  values of the prepared composites, elemental lead and PES are given in Table 5.

According to results, the  $\mu_M$  values of the composites became independent from the type of used reinforcement for intermediate and high energy regions in accordance with the changing dominant interaction mechanisms in different energies regions. For the low energy region, composites with denser electron density have been found to have higher  $\mu_M$

values because of the photoelectric interaction. The  $\mu_M$  values of the prepared composites and elemental lead are also compared by using mean  $\mu_M$  values for low, intermediate and high IEMR energy regions in Fig. 14.

The heaviest composite produced in this study is approximately 5.5 times lighter than lead. Thus although  $\mu_L$  values of lead was higher than the composites  $\mu_M$  values of lead was lower than nearly all the composites.

### Half value layer (HVL) values of the composites

The determined HVL values, that is the thickness of the material at which the intensity of radiation entering is reduced by one half, are given for the prepared composites, elemental lead and PES in Table 6.

**Fig. 4** FTIR spectra of the PES and 50% reinforced composites

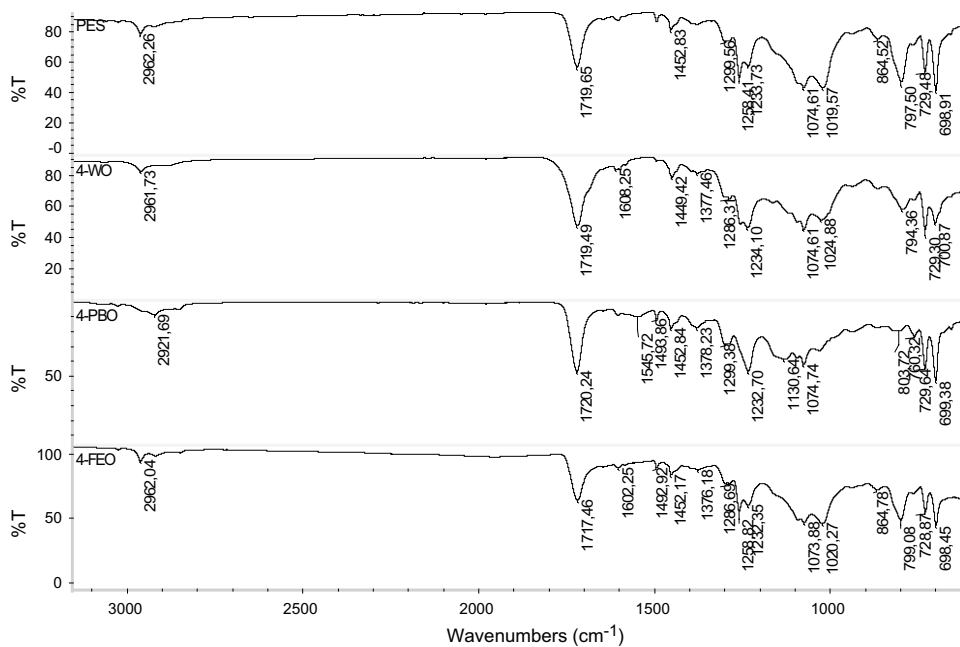
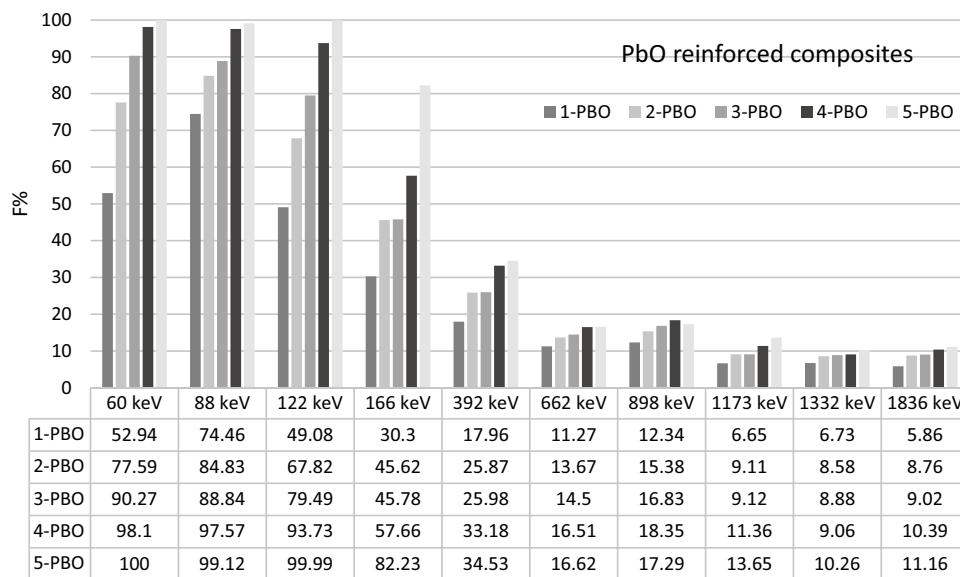


**Fig. 5** F% values of PbO reinforced composites at different IEMR energies



Although high thickness is a disadvantage for wearable shields, produced composites were still lighter than lead for the same shielding performance. For low IEMR energy region 5-PBO composite reached approximately 84.6% performance of lead. According HVL values, a 5-PBO shield that is approximately 3.6 times thicker than lead shield would perform the same attenuation performance with lead shield, and its total mass would still be approximately 1.5 times less than lead shield even in this thickness. For intermediate and high energy regions 5-FEO composite reached approximately 29.8% and approximately 31.3% performance of lead, respectively. This composite would perform the same attenuation performance with lead shield

when it is approximately 4.7 times thicker (for intermediate energies) and approximately 4.00 times thicker (for high energies) than a lead shield. Although it is used thicker it would still be approximately 1.3 times lighter at low energy region and approximately 1.5 times lighter at high energy region.

### Conclusions

In the study, all the reinforcement particles were observed to disperse uniformly in the PES matrix. Composites exhibited good IEMR shielding properties especially for high filler

**Fig. 6** F% values of WO<sub>3</sub> reinforced composites at different IEMR energies

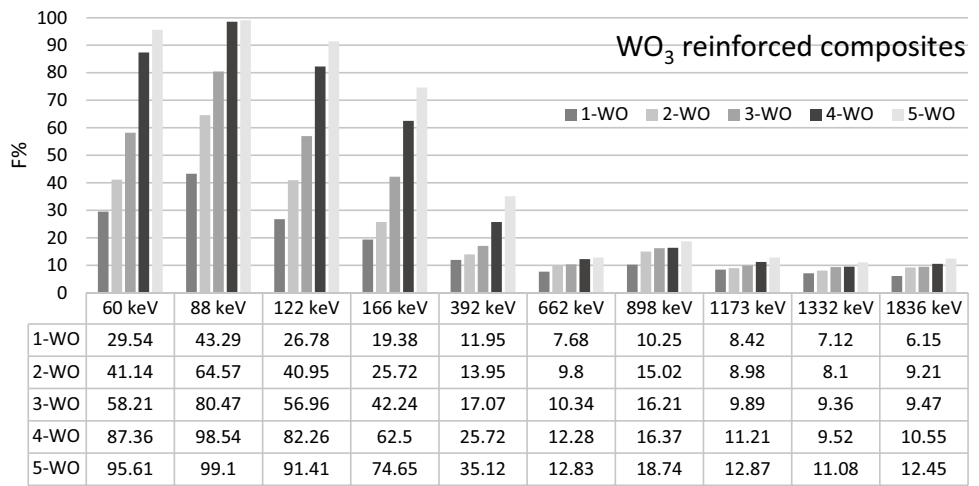


**Fig. 7** F% values of Fe<sub>3</sub>O<sub>4</sub> reinforced composites at different IEMR energies

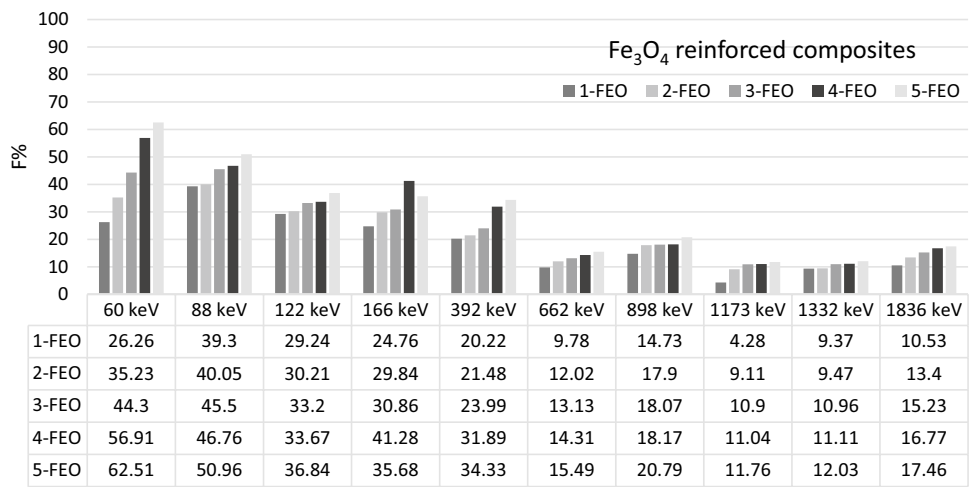


**Fig. 8** Plot of linear dependence of  $\mu_L$  values on density of PbO reinforced filled composites

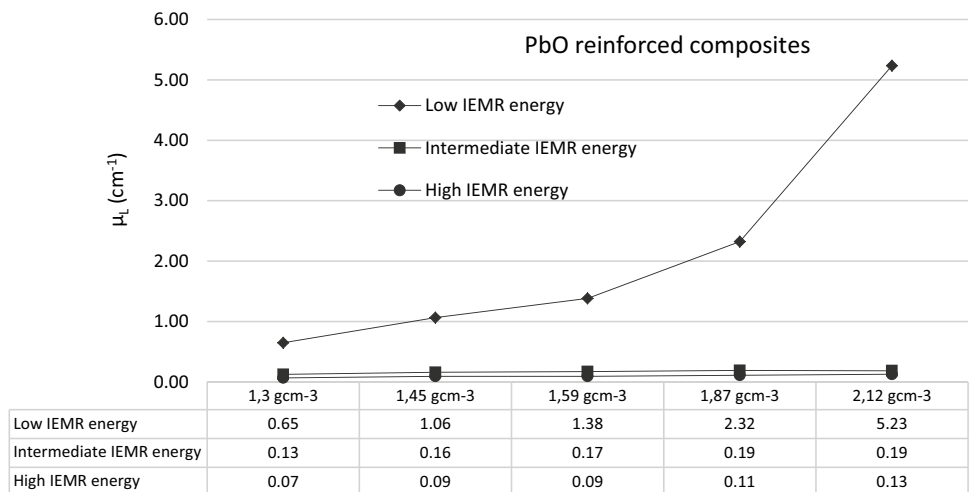




**Fig. 9** Plot of linear dependence of  $\mu_L$  values on density of  $WO_3$  reinforced filled composites

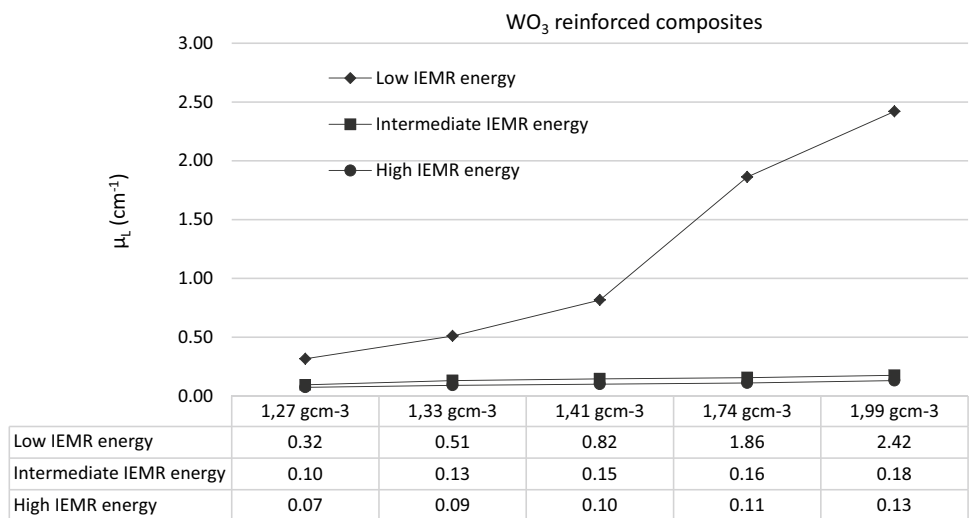


**Fig. 10** Plot of linear dependence of  $\mu_L$  values on density of  $Fe_3O_4$  reinforced filled composites

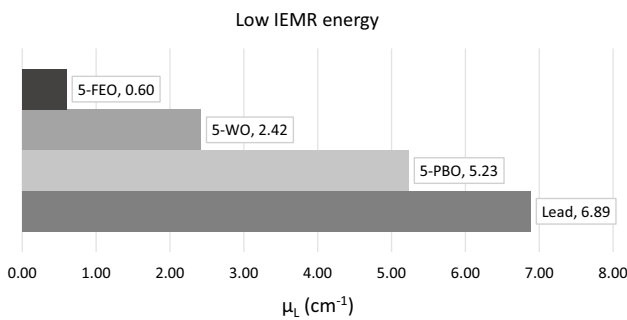
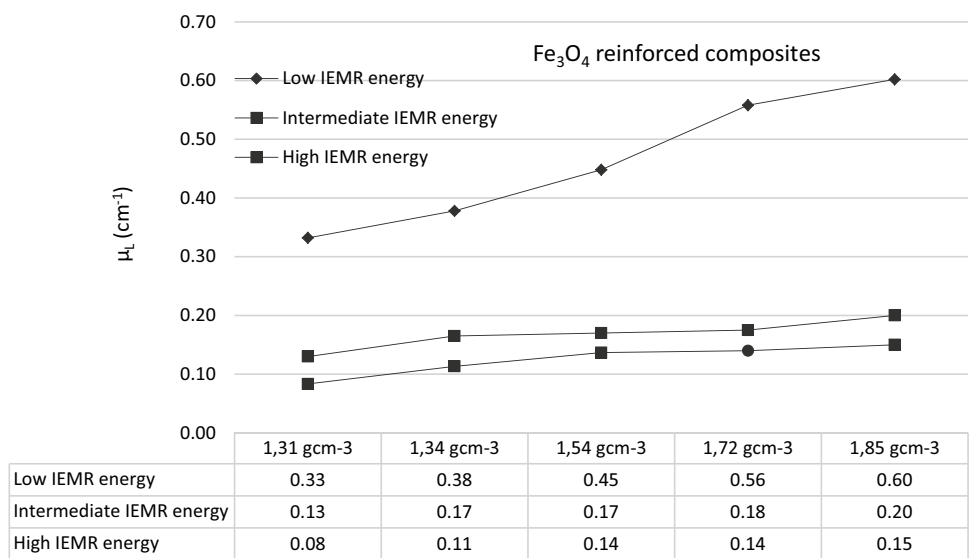


**Fig. 11**  $\mu_L$  values of composites and lead for low IEMR energy region

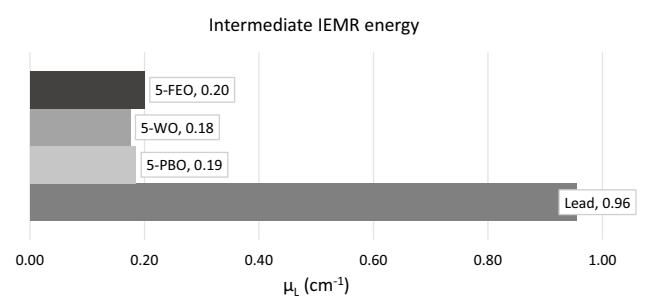


**Fig. 12**  $\mu_L$  values of composites and lead for intermediate IEMR energy region

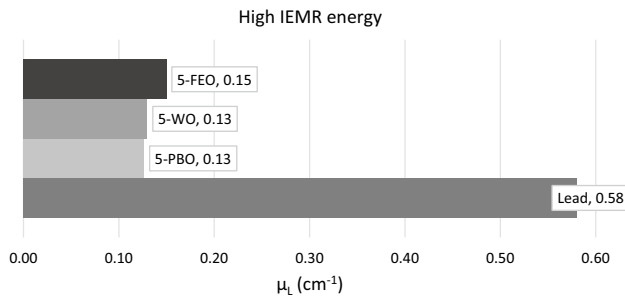


**Fig. 13**  $\mu_L$  values of composites and lead for high IEMR energy region

loadings and low energies. The density of the composites influenced the IEMR shielding performances of the composites for low IEMR energies significantly but as the IEMR energy was raised the density effect on IEMR shielding performances became ineffective.

Thus especially when weight of IEMR shield is important these composites are superior to lead by virtue of their light weight. Their non-toxic nature is also another important advantage of them.

**Table 5** Determined  $\mu_M$  values of the prepared composites, elemental lead and PES

Sample designation	Low IEMR energy					Intermediate IEMR energy		High IEMR energy		
	60 keV	88 keV	122 keV	166 keV	392 keV	662 keV	898 keV	1173 keV	1332 keV	1836 keV
$\mu_M$ ( $\text{cm}^2\text{g}^{-1}$ )										
Lead	0.90	0.36	0.80	0.75	0.23	0.10	0.07	0.06	0.05	0.04
1-PBO	0.58	1.05	0.52	0.28	0.07	0.09	0.10	0.05	0.05	0.05
2-PBO	1.03	1.30	0.78	0.42	0.13	0.10	0.12	0.07	0.06	0.06
3-PBO	1.47	1.38	1.00	0.39	0.12	0.10	0.12	0.06	0.06	0.06
4-PBO	2.12	1.99	1.48	0.46	0.16	0.10	0.11	0.06	0.05	0.06
5-PBO	4.81	2.23	4.29	0.81	0.20	0.09	0.09	0.07	0.05	0.06
1-WO	0.28	0.45	0.25	0.17	0.10	0.06	0.09	0.07	0.06	0.05
2-WO	0.40	0.78	0.40	0.22	0.11	0.08	0.12	0.07	0.06	0.07
3-WO	0.62	1.16	0.60	0.39	0.13	0.08	0.13	0.07	0.07	0.07
4-WO	1.19	2.43	0.99	0.56	0.17	0.08	0.10	0.07	0.06	0.06
5-WO	1.57	2.36	1.23	0.69	0.22	0.07	0.10	0.07	0.06	0.07
1-FEO	0.23	0.38	0.26	0.22	0.17	0.08	0.12	0.03	0.07	0.08
2-FEO	0.32	0.38	0.27	0.26	0.18	0.10	0.15	0.07	0.07	0.11
3-FEO	0.38	0.40	0.26	0.24	0.18	0.09	0.13	0.08	0.08	0.11
4-FEO	0.49	0.37	0.24	0.31	0.22	0.09	0.12	0.07	0.07	0.11
5-FEO	0.53	0.38	0.25	0.24	0.23	0.09	0.13	0.07	0.07	0.10

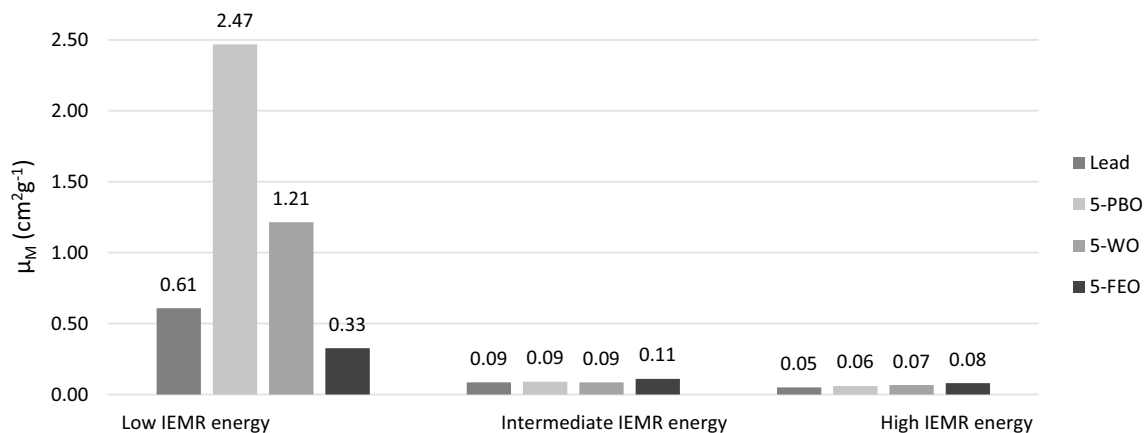


**Fig. 14**  $\mu_M$  values of the prepared composites and elemental lead

**Table 6** Determined HVL values of the prepared composites, elemental lead and PES

Sample designation	Low IEMR energy					Intermediate IEMR energy		High IEMR energy		
	60 keV	88 keV	122 keV	166 keV	392 keV	662 keV	898 keV	1173 keV	1332 keV	1836 keV
HVL (cm)										
Lead	0.07	0.17	0.08	0.08	0.26	0.61	0.89	1.1	1.15	1.37
PES	3.82	2.88	3.43	3.47	3.78	6.1	4.15	8.75	8.01	6.19
1-PBO	0.92	0.51	1.03	1.92	7.45	5.8	5.26	10.08	9.95	11.48
2-PBO	0.46	0.37	0.61	1.14	3.56	4.71	4.15	7.26	7.73	7.56
3-PBO	0.3	0.32	0.44	1.13	3.54	4.42	3.76	7.24	7.45	7.33
4-PBO	0.17	0.19	0.25	0.81	2.32	3.84	3.42	5.75	7.29	6.32
5-PBO	0.07	0.15	0.08	0.4	1.64	3.81	3.65	4.72	6.4	5.85
1-WO	1.98	1.22	2.22	3.22	5.44	8.67	6.41	7.88	9.38	10.92
2-WO	1.31	0.67	1.32	2.33	4.61	6.72	4.26	7.36	8.2	7.17
3-WO	0.79	0.42	0.82	1.26	3.7	6.35	3.92	6.66	7.05	6.96
4-WO	0.34	0.16	0.4	0.71	2.33	5.29	3.88	5.83	6.92	6.22
5-WO	0.22	0.15	0.28	0.5	1.6	5.05	3.34	5.03	5.9	5.21
1-FEO	2.28	1.39	2	2.44	3.07	6.73	4.35	15.84	7.04	6.23
2-FEO	1.6	1.35	1.93	1.96	2.87	5.41	3.51	7.26	6.97	4.82
3-FEO	1.18	1.14	1.72	1.88	2.53	4.93	3.48	6	5.97	4.19
4-FEO	0.82	1.1	1.69	1.3	1.8	4.49	3.46	5.93	5.88	3.78
5-FEO	0.71	0.97	1.51	1.57	1.65	4.12	2.97	5.54	5.41	3.61

**Acknowledgements** The authors would like to acknowledge the financial assistance of the Mugla Sitki Kocman University through the Grant 2014/003 February 2014.

## References

- El-Sayed Abdo A, El-Sarraf MA, Gaber FA (2003) Utilization of ilmenite/epoxy composite for neutrons and gamma rays attenuation. *Ann Nucl Energy* 30:175–187
- Plionis AA, Garcia SR, Gonzales ER, Porterfield DR, Peterson DS (2009) Replacement of lead bricks with non-hazardous polymer-bismuth for low-energy gamma shielding. *J Radioanal Nucl Chem* 282:239–242
- Gwaily SE, Madani M (2002) Lead-natural rubber composites as gamma radiation shields. II: High concentration. *Polym Compos* 23:495–499
- Mheemeed AK, Hasan HI, Al-Jomaily FM (2012) Gamma-ray absorption using rubber-lead mixtures as radiation protection shields. *J Radioanal Nucl Chem* 291:653–659
- Harish V, Nagaiah N, Niranjana Prabhu T, Varughese KT (2009) Preparation and characterization of lead monoxide filled unsaturated polyester based polymer composites for gamma radiation shielding applications. *J Appl Polym Sci* 112:1508–1530
- Korpinar B, Ozturk BC, Cam NF, Akat H (2020) Radiation shielding properties of poly(hydroxyethyl methacrylate)/Tungsten(VI) oxide composites. *Mater Chem Phys* 239:121986
- Higgins MCM, Radcliffe NA, Toro-Gonzales M, Rojas JV (2019) Gamma ray attenuation of hafnium and tungsten trioxide-epoxy resin composites. *J Radioanal Nucl Chem* 332:707–716
- Muthamma MV, Bubbly SG, Gudennavar SB, Narendranath KCS (2019) Poly(vinyl alcohol)-bismuth oxide composites for X-ray and gamma ray shielding applications. *J Appl Polym Sci* 136:47949
- Abdalsalam AH, Sayyed MI, Hussein TA, Sakar E, Mhareb MHA, Sakar BC, Alim B, Kaky KM (2019) A study of gamma attenuation property of UHMWPE/Bi<sub>2</sub>O<sub>3</sub> nanocomposites. *Chem Phys* 523:92–98
- Tijani SA, Al-Hadeethi Y (2019) The use of isophthalic-bismuth polymer composites as radiation shielding barriers in nuclear medicine. *Mater Res Express*. 6:055323
- Avcioglu S, Buldu M, Kaya F, Ustundag CB, Kam E, Menciloglu YZ, Kaptan HY, Kaya C (2020) Processing and properties of boron carbide (B<sub>4</sub>C) reinforced composites for radiation shielding. *Ceram Int* 46:343–352
- Banerjee P, Bhattacharjee Y, Bose S (2020) Lightweight epoxy-based composites for EMI Shielding Applications. *J Electron Mater* 49:1702–1720
- Eren Belgin E, Aycik GA (2015) Preparation and radiation attenuation performances of metal oxide filled polyethylene based composites for ionizing electromagnetic radiation shielding applications. *J Radioanal Nucl Chem* 306:107–117
- Eren Belgin E, Aycik GA, Kalemantas A, Pelit A, Dilek DA, Kavak MT (2015) Preparation and characterization of a novel ionizing electromagnetic radiation shielding material; hematite filled polyester based composites. *Radiat Phys Chem* 115:43–48
- Eren Belgin E, Aycik GA, Kalemantas A, Pelit A, Dilek DA, Kavak MT (2016) Usability of natural titanium-iron oxide as filler material for ionizing electromagnetic radiation shielding composites; preparation, characterization and performance. *J Radioanal Nucl Chem* 309:659–666
- Friedlander G, Kennedy JW, Macias ES, Miller JM (1981) *Nucl Radiochem*, 3rd edn. Wiley, New York

**Publisher's Note** Springer Nature remains neutral with regard to jurisdictional claims in published maps and institutional affiliations.